

Edge-flames in circular channels: Multiplicity of steady-state axisymmetric solutions

Vadim N. Kurdyumov*, Carmen Jiménez

Department of Energy, CIEMAT, Avda. Complutense 22, 28040 Madrid, Spain

ARTICLE INFO

Keywords:

Edge flame
Diffusion flame
Multiplicity of solutions
Mixing layer

ABSTRACT

A numerical study of the combustion process occurring after separate injection of fuel and oxidizer through an end-wall porous plug into a semi-infinite circular channel is presented. The fuel flow is injected into the center of the channel, surrounded by the oxidizer flow in an axisymmetric manner. It is assumed that the channel walls and the porous plug are kept at constant (cold) temperature. The study is based on the coupled Navier–Stokes and transport equations with one-step Arrhenius-type combustion kinetics. The structure of the combustion field consists of an edge flame located in the reactants mixing layer and a diffusion flame following it.

The study is limited to finding axisymmetric solutions. It is found that, for certain values of the parameters, the system can have multiple (up to four) axisymmetric solutions. Particular attention is paid to finding the bifurcation points bounding these multiple solution regions in parametric space. It is shown that in all likelihood the effect of the fuel Lewis number, Le_F , is decisive for the emergence of multiple modes. For $Le_F = 1$ only two modes appear, while with a decrease in Le_F the number of modes can increase to four. Although the analysis of the stability of the different regimes remains outside the scope of this work, the shape of the curve relating the flame position to the reaction Damköhler number suggests that only two of them can be simultaneously stable.

Novelty and significance statement: This paper presents a numerical investigation of the edge flame solutions obtained after injection of a central fuel jet surrounded by air in a circular channel, showing for the first time that multiple axisymmetric steady-state solutions can exist. For fuels with Lewis number equal to one two solutions are generally found, with only one being stable. For fuels with smaller Lewis numbers the number of solutions is increased up to four solutions, where two of them can be simultaneously stable. This may explain the alternance of anchored and lifted flames in axial non-premixed burners burning hydrogen reported in experiments.

1. Introduction

The separate injection of fuel and oxidizer into a combustion chamber has an obvious advantage over injection of a premixed reactive mixture: the flame cannot propagate upstream along the supply channel. The possibility of occurrence of this dangerous event known as the flashback effect must always be taken into account when designing combustion devices.

When the initially separated streams of fuel and oxidizer come into contact and are ignited a well-known structure called an edge flame is formed [1–4]. The study of this structure is of decisive importance, since it is the leading point of a diffusion flame situated behind, thus determining the dynamics of the combustion process and the flame stabilization and extinction conditions.

One of the most widely studied configurations is the situation where the streams of fuel and oxidizer are initially separated by a semi-infinite splitter plate and the edge flame is stabilized downstream the tip of the plate [5–12]. The structure of steady-state edge flames in the case of separate fuel and oxidizer injection from a porous plug was considered in [13], where one-stage kinetics for methane combustion was used. The structure and dynamics of edge flames with varying fuel Lewis numbers during injection of fuel and oxidizer from mutually perpendicular porous plugs was considered in [14]. A propagating edge-flame is another possible configuration, formed after ignition along the contact surface of the fuel and oxidizer [15–22]. In this case, the edge flame velocity is an eigenvalue of the problem that needs to be calculated simultaneously.

* Corresponding author.

E-mail address: vadim.k@ciemat.es (V.N. Kurdyumov).

<https://doi.org/10.1016/j.combustflame.2024.113433>

Received 2 January 2024; Received in revised form 23 March 2024; Accepted 25 March 2024

0010-2180/© 2024 The Author(s). Published by Elsevier Inc. on behalf of The Combustion Institute. This is an open access article under the CC BY license (<http://creativecommons.org/licenses/by/4.0/>).

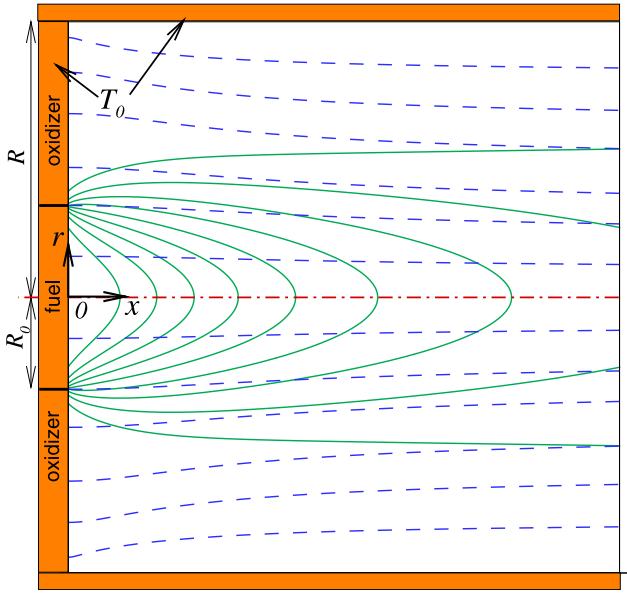


Fig. 1. Sketch of the problem, coordinate system, distributions of the normalized mass fraction of fuel (solid isolines, with an interval of 0.1) and the stream function plotted for $m = 10$ and non-reacting flow ($D = 0$).

A single edge flame was considered in all the above studies. However, it is obvious that in a more realistic situation, several edge flames can coexist. An example is the injection of reactants in a combustion chamber in the form of multiple streams. In this case, the thermal interaction between neighboring edge flames is inevitable, leading to new effects thus complicating the understanding of the resulting flame structure.

Perhaps the first systematic attempt to study the interaction of multiple edge flames was reported in [23], where the interaction of two edge flames was investigated within the framework of a constant density model for a planar jet injection configuration. As an extension, thermal expansion was taken into account in [24], a study based in the full Navier–Stokes equations (including heat expansion effects) also for the planar injection case. The main result obtained in [23,24] was the discovery of a multiplicity of combustion modes under the same values of the control parameters and corresponding to different flame structures. It was also found that several modes can be simultaneously stable and the actual implementation of each of them depends on the initial ignition conditions.

The investigation of steady-state combustion modes for injection of a circular fuel jet based on the numerical simulation of the Navier–Stokes equations is proposed in the present work. Since modeling a 3D process is rather expensive from the point of view of computation, the present study is limited to axisymmetric cases. Experimental evidence of the existence of a multiplicity of steady-state regimes in a system resembling this one was recently demonstrated in [25]. The main emphasis is on detecting the existence and studying the boundaries of the multiplicity regions, which requires the calculation of both stable and unstable solutions. Despite the limitations caused by the axisymmetric assumption, this investigation can be considered as a first step towards studying more general three-dimensional flame structures.

2. Formulation

Fuel and oxidizer are injected in separate streams through a porous plug at the end of a cylindrical semi-infinite channel of radius R . The fuel is injected through a circular section of radius R_0 located at the center of the porous plug, and the oxidizer is injected through the remaining porous surface. It is assumed that the fuel and oxidizer

do not mix inside the porous plug. The gas streams emerge from the porous surface with the same uniform normal velocity U . In this study, we are looking for axisymmetric solutions exclusively, so that all distributions of variables depend only on the longitudinal variable x along the channel axis and the radial variable r . The sketch of the problem for a situation without combustion is given in Fig. 1, where the solid contours show the fuel mass fraction distribution and the dashed contours represent the stream function. It can be seen that despite the uniform injection of gas, a boundary layer is formed near the channel wall due to the no-slip velocity condition on it.

The thermal conductivity of the plug volume is assumed to be sufficiently high so as to maintain the gas temperature at the porous plug exit uniform and equal to T_0 . The impermeable channel walls are kept at the same temperature, T_0 . At the exit of the plug the reactants mass fraction fluxes are specified. An axisymmetric mixing layer, along which the reactants interdiffuse, is produced downstream the porous plug surface.

In this study we model the chemical reaction by a global one step irreversible reaction of the form: $F + sO \rightarrow (1 + s)P$, where F and O denote fuel and oxidizer, P denotes combustion products and s is the mass-weighted stoichiometric coefficient. The fuel consumption rate per unit volume is assumed to be first order in the concentrations of the two reactants, $(\rho Y_F/W_F)$ and $(\rho Y_O/W_F)$, and to obey a standard Arrhenius law, $\Omega = B\rho^2 Y_F Y_O \exp(-\mathcal{E}/RT)$, with a preexponential factor B (containing the molecular weights) and an overall activation energy \mathcal{E} . Here Y_F and Y_O are the mass fractions of fuel and oxidizer, respectively, T and ρ are the temperature and density of the mixture, and \mathcal{R} is the universal gas constant.

In writing the dimensionless governing equations below, the initial radius of the fuel stream, R_0 , was chosen as a unit of length, the characteristic velocity D_T/R_0 as a unit of speed and R_0^2/D_T as a unit of time; here D_T is the thermal diffusivity of the mixture. The mixture density ρ and the mass fractions Y_F, Y_O were normalized with respect to their values in the supply streams, ρ_0 and Y_{F_0}, Y_{O_0} , and a non-dimensional temperature $\theta = (T - T_0)/(T_a - T_0)$ was introduced, where $T_a = T_0 + QY_{F_0}/[c_p(1 + \phi)]$ is the adiabatic temperature with Q the heat release rate (per unit mass of fuel), $\phi = sY_{F_0}/Y_{O_0}$ is the global fuel-to-oxidizer equivalence ratio and c_p is the specific heat.

For the sake of simplicity of the formulation, all the thermodynamic and transport coefficients are assumed to be constant. Assuming a low-Mach number approximation, the standard (dimensionless) steady-state governing equations become

$$\nabla \cdot \rho \mathbf{v} = 0, \quad (1)$$

$$(\rho \mathbf{v} \cdot \nabla) \mathbf{v} = -\nabla p + Pr(\nabla^2 \mathbf{v} + \nabla(\nabla \cdot \mathbf{v})/3), \quad (2)$$

$$\rho \mathbf{v} \cdot \nabla \theta = \nabla^2 \theta + (1 + \phi)\omega, \quad (3)$$

$$\rho \mathbf{v} \cdot \nabla Y_F = Le_F^{-1} \nabla^2 Y_F - \omega, \quad (4)$$

$$\rho \mathbf{v} \cdot \nabla Y_O = Le_O^{-1} \nabla^2 Y_O - \phi \omega, \quad (5)$$

$$\rho(1 + q\theta) = 1, \quad (6)$$

where $\mathbf{v} = u\mathbf{e}_x + v\mathbf{e}_r$ is the velocity vector with u and v the corresponding axial and radial velocity components. The heating effect due to viscous dissipation is neglected due to its insignificance compared to the heat released by combustion in the above equations.

The boundary conditions at the porous plug exit surface, $x = 0$, are

$$\begin{aligned} \rho = 1, \quad \theta = 0, \quad u = m, \quad v = 0, \\ mY_F - \frac{1}{Le_F} \frac{\partial Y_F}{\partial x} = \begin{cases} m, & r < 1 \\ 0, & r > 1 \end{cases} \\ mY_O - \frac{1}{Le_O} \frac{\partial Y_O}{\partial x} = \begin{cases} 0, & r < 1 \\ m, & r > 1 \end{cases} \end{aligned} \quad (7)$$

Here it is assumed that injection occurs in the direction normal to the porous surface. Downstream of the channel, at $x \rightarrow \infty$, we impose for the temperature, species mass fractions and velocity components the following conditions,

$$\frac{\partial^2 \theta}{\partial x^2} = \frac{\partial^2 Y_F}{\partial x^2} = \frac{\partial^2 Y_O}{\partial x^2} = \frac{\partial u}{\partial x} = v = 0. \quad (8)$$

These conditions, which are typical soft boundary conditions, were applied at the outlet boundary of the numerical domain. It was verified that they are not affecting the results (by changing the length of the computational domain).

The channel wall, at $r = a$, is isothermal, impermeable for fuel and oxidizer with no-slip conditions for the gas velocity

$$\theta = 0, \quad \frac{\partial Y_F}{\partial r} = \frac{\partial Y_O}{\partial r} = 0, \quad u = v = 0. \quad (9)$$

The dimensionless parameters in Eqs. (1)–(7) are the Prandtl number $Pr = \nu/D_T$, where ν and D_T are the kinematic viscosity and the thermal diffusivity, the scaled injection velocity of the gas $m = UR_0/D_T$, the channel radius $a = R/R_0$, the Lewis numbers associated with the fuel and oxidizer $Le_F = D_T/D_F$ and $Le_O = D_T/D_O$, where D_F and D_O are the molecular diffusivities of the fuel and oxidizer, respectively, and the thermal expansion parameter $q = (T_a - T_0)/T_0$.

The dimensionless Arrhenius reaction rate is given by

$$\omega = D\beta^3 \rho^2 Y_F Y_O \exp\left[\frac{\beta(\theta - 1)}{(1 + q\theta)/(1 + q)}\right], \quad (10)$$

where $\beta = \mathcal{E}(T_a - T_0)/RT_a^2$ and $D = (R_0^2/D_T) \cdot B\rho_0 Y_{O_0} \beta^{-3} \exp[-\mathcal{E}/RT_a]$ are the Zel'dovich and Damköhler numbers, respectively.

When choosing dimensionless parameters for a combustion process, the dimensionless activation energy, $N = \mathcal{E}/RT_0$, is often used instead of the Zel'dovich number. Because $\beta = Nq/(1 + q)^2$, an increase in the Zel'dovich number occurs with a decrease in q (at a fixed activation energy \mathcal{E}), that is, for leaner mixtures. Due to the significant number of parameters appearing in the problem, we fix the values $q = 5$ and $Pr = 0.72$, which are typical values for combustible mixtures. Also, for all the results presented below we use $Le_O = 1$ and $\phi = 1$.

Only axisymmetric solutions are considered in the present study. The edge flame position is determined as the point (x_w, r_w) at which the reaction rate ω reaches a local maximum value, $\omega_{max} = \omega(x_w, r_w)$.

3. Numerical treatment

It is advantageous for two-dimensional steady-state numerical simulations to eliminate the pressure from the momentum equations by introducing the vorticity field, $\zeta = v_x - u_r$. Subscripts x and r , here and below, denote partial differentiations. The vorticity satisfies

$$\rho v \cdot \nabla \zeta - \rho v \zeta / r = Pr(\Delta \zeta - \zeta/r^2) + J, \quad (11)$$

where J is the vorticity production term given by

$$J = v_x(\rho v)_r - v_r(\rho v)_x + u_x(\rho u)_r - u_r(\rho u)_x.$$

The continuity equation is satisfied automatically by introducing a stream function ψ , defined from $r\rho u = \psi_r$, $r\rho v = -\psi_x$, which satisfies

$$(\rho^{-1}\psi_x)_x + (\rho^{-1}\psi_r)_r - (\rho r)^{-1}\psi_r = -r\zeta \quad (12)$$

The solutions described by Eqs. (3)–(6) and (11)–(12) were calculated using the Gauss–Seidel method with over-relaxation. The typical step size of the uniform square numerical grid was $h = 0.02$. It was verified that increasing the resolution to $h = 0.01$ did not lead to changes in the results. Two versions of the calculations were carried out. In the first case, direct iterative calculations of all distributions were performed with fixed values for all parameters. In the second case, the temperature value, $\theta = \theta_*$, was fixed at one point of the domain while the value of the Damköhler number, D , was calculated iteratively also by the Gauss–Seidel method with over-relaxation.

The choice of the temperature θ_* and its location had to correspond to some real solution (stable or unstable). To ensure this, a previously calculated solution was shifted by several grid points downstream/upstream and used as the initial condition for iterations. The typical values for θ_* were between 0.7 and 0.8 fixed in a point along the $r = r_*$ line with $r_* \lesssim 1$. Numerical calculations revealed that the best convergence was achieved when the value of r_* was close to the radial value of the corresponding edge flame position r_w . For this reason, the values of r_* were gradually decreased as the flame edge moved away from the porous plug (which led to the flame edge approaching the channel axis, see Fig. 4). However, it was verified that the solution obtained after the iterative calculations does not depend on the values of θ_* and r_* (within reasonable limits).

4. Results

Let us first consider the case with fuel Lewis number equal to one, $Le_F = 1$. Fig. 2 shows on the left plot the edge flame position as a function of the Damköhler number, while on the right plot, $\beta^3 D$ is used for the horizontal axis. The comparison of these two plots illustrates the importance of introducing β^3 as a factor, into the expression for the dimensionless reaction rate given by Eq. (10). Indeed, the response curves on the left plot turn out to be much closer to each other at different β (or, equivalently N) than on the right plot. The scaling of the Damköhler number with β^3 reflects the fact that the flame edge is located at the stoichiometric line.

Fig. 2 shows that the response curve consists of two branches. The edge flame position approaches the porous plug as the Damköhler number increases along the lower branch, while x_w increases with D along the upper branch. The two branches are connected at a bifurcation point (open circles) which determines the critical value for the Damköhler number, $D = D_c$. There are no solutions for $D < D_c$. Although the investigation of the stability of the computed steady-states remains beyond the scope of this work, one can be sure that the lower branch of the response curve describes stable solutions, while along the upper branch the steady-state solutions are unstable. We will call the first type of solutions (when x_w decreases as D increases) as “normal” solutions, according to the intuitive consideration that the flame should approach the porous plug as the intensity of the reaction increases.

A similar behavior was obtained in [24], where the structure of the edge flames after separate injection of fuel and air in a planar channel was considered. Numerical simulations of the corresponding time-dependent dynamics showed that the “normal” regimes are stable (small perturbations of these solutions decrease with time). However, a rigorous linear global analysis of the stability of stationary solutions is a challenging task and will be reported elsewhere.

An analogy can be established between the “C”-curves presented here and those obtained when considering a freely propagating premixed flame in a channel with heat losses to the wall. In the last case, two branches of steady-state solutions are also observed: a stable one, corresponding to a decrease in the propagation flame velocity (relative to the wall) with increasing heat loss intensity, and another solution in which the flame velocity increases with increasing heat losses.

The behavior of the response curve becomes more complex as the Lewis number for the fuel decreases. Fig. 3 shows the dependence of the flame position on the Damköhler number for varying flow rate values m . All curves are calculated for $Le_F = 0.7$. It can be seen that at a relatively small flow rate, $m = 6$, the response curve resembles those shown in Fig. 2 for $Le_F = 1$, with two solutions for any Damköhler number above D_c (marked with an open triangle) and no solutions for $D < D_c$.

The situation changes as the flow rate increases. It can be seen in Fig. 3 that for the cases calculated with $m = 8$ and $m = 10$, two additional bifurcation points appear on the response curves. These bifurcation points (marked with open triangles) are indicated as (b) and (c) on the curve with $m = 10$, in addition to bifurcation point (a). Thus,

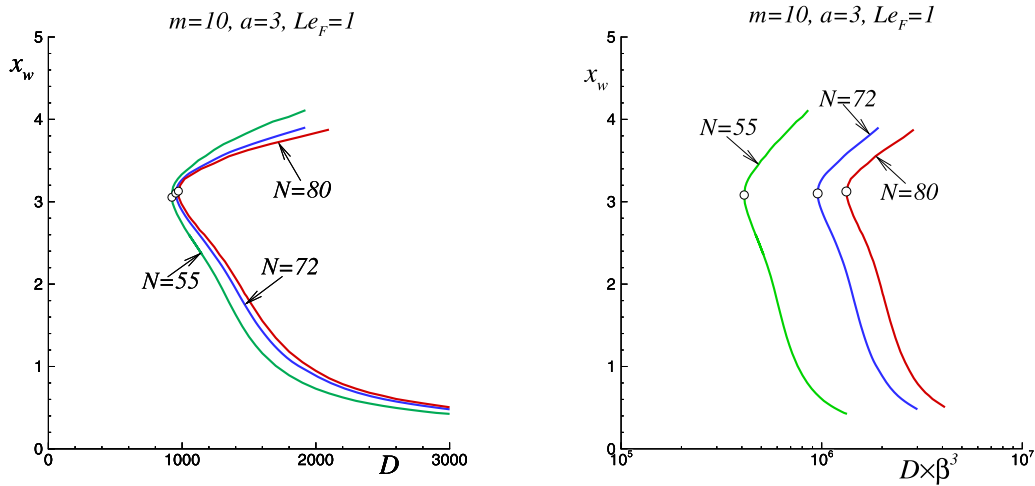


Fig. 2. Dependence of the edge flame position on the Damköhler number calculated for $m = 10$, $q = 5$ and $Le_F = 1$ at different values of the dimensionless activation energy N . The left plot shows the flame position as a function of the Damkohler number and the right plot as a function of $D\beta^3$, where $\beta = qN/(1+q)^2$. Bifurcation points are marked with open circles.

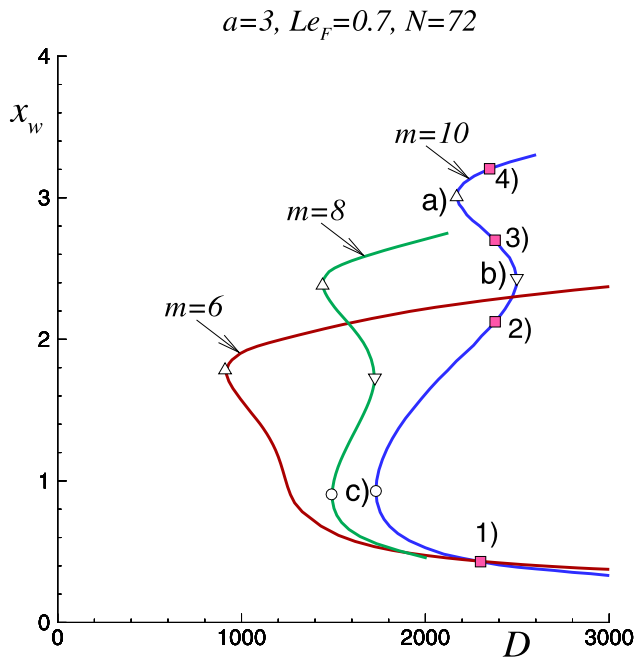


Fig. 3. Dependence of the edge flame position on the Damköhler number calculated for several flow rates m ; with $a = 3$, $N = 72$, $q = 5$ and $Le_F = 0.7$. Bifurcation points are marked with open symbols. The filled squares on the curve with $m = 10$ correspond to the solutions in Fig. 4.

for a fixed Damköhler number, up to four steady-state solutions can exist for the same set of parameters. It should be noted that between points (a) and (b), the position of the flame edge x_w also decreases with increasing Damköhler number and solutions along this segment of the response curve are “normal” and in all probability stable.

Fig. 4 illustrates the temperature distributions (colored shades), the reaction rate isolines (black lines) and the stream function isolines (white lines) for the solutions shown as filled squares (1), (2) (3) and (4) on the curve with $m = 10$ in Fig. 3. It can be seen that, as the flame shifts away from the porous plug, the position of the edge moves closer to the center of the channel and the circle formed by the axisymmetric edges can even blend into a single edge at the channel axis. As stated above, in all probability only solutions (1) and (3) are stable.

Fig. 5 shows the response curves as a function of the Damköhler number calculated for different values of Le_F , for $m = 10$, $a = 3$ and $N = 72$. As mentioned above, for $Le_F \geq 1$ only two modes are observed. As the Lewis number gradually decreases (for a fixed flow rate), additional turning points appear and the response curve becomes double C-shaped. The interval of existence of four solutions slightly increases with a decreasing Lewis number.

The curves shown in Fig. 6 illustrate the dependence of the flame edge position on the Damköhler number obtained for $m = 10$, $a = 3$ and $Le_F = 0.7$ and several values of the activation energy N . It should be noted that for the solutions located closest to the porous plug, all the curves practically overlap. However, for solutions with edge flame positions more distant from the porous plug, the separation between the curves for different N increases with x_w . One can see also that the region of existence of four solutions decreases as the dimensionless activation energy decreases. For very small values of N , e.g. the response curve calculated for $N = 20$, the region of four solutions does not exist.

All the results presented above were obtained for a dimensionless channel radius $a = 3$. As can be seen in Fig. 4, the combustion field, even at this value of a , does not extend far from the axis. However, due to thermal expansion, the gas velocity behind the edge flame increases to different degrees at different values of a . Fig. 7 compares the distributions of the longitudinal velocity field u (color shades) and the reaction rate isolines ($\omega = 0.5, 1, 5, 20, 50$) for the cases calculated with $a = 2$ and $a = 5$. It can be seen that although the positions of the edge flame are close to each other, the velocity fields are noticeably different. On the other hand, it should be noted that the flame structures (ω reaction rate isolines) are very similar for $a = 2$ and $a = 5$.

Fig. 8 shows the velocity profiles along the channel axis calculated for $D = 2300$, $m = 10$, $Le_F = 0.7$ and different values of the channel radius a . It can be seen that with an increase in a , the maximum values of the gas velocity achieved after the edge flame decrease appreciably. It should be noted that for the cold wall cases considered in the present study, the temperature of the combustion products will asymptotically drop to zero far downstream and the velocity distribution should approach the well-known parabolic Poiseuille profile, $u \rightarrow 2m[1-(r/a)^2]$ as $x \rightarrow \infty$, that is, $u|_{r=0} \rightarrow 2m$. However, this limit value is reached only at $x \gg 1$.

A quantitative change in the gas flow velocity distribution entails a change in the bifurcation points for the response curves. Fig. 9 shows the response curves obtained for several values of a , all curves calculated for $m = 10$, $N = 72$ and $Le_F = 0.7$. It should be noted,

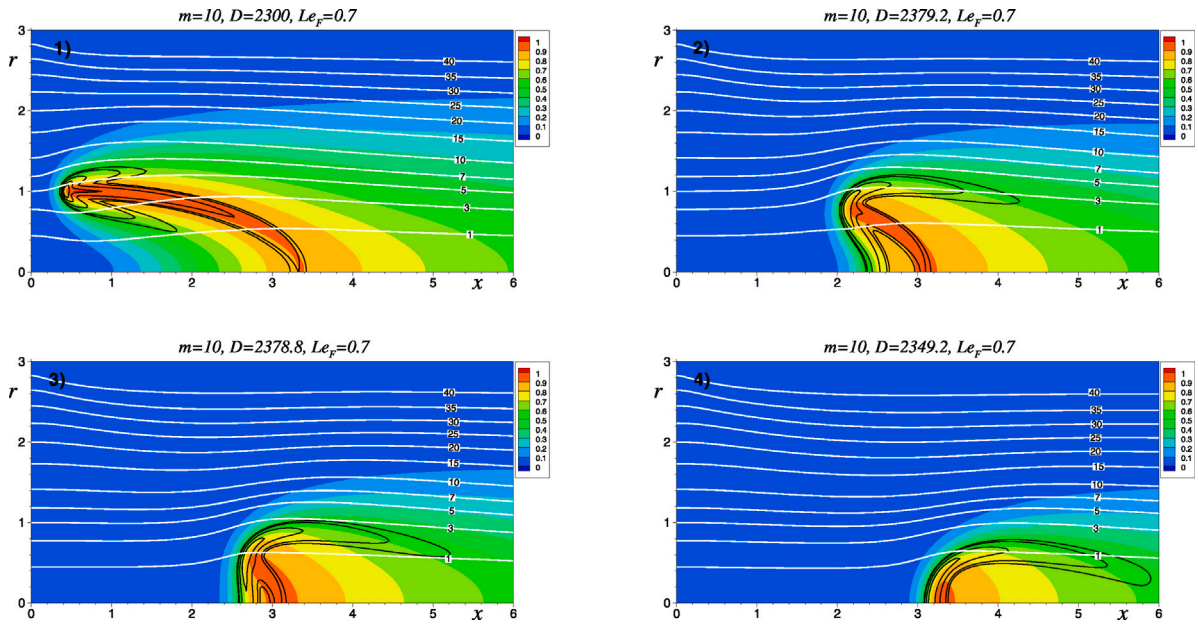


Fig. 4. Example of the four flame solutions obtained for $m = 10$, $a = 3$, $N = 72$ and $Le_F = 0.7$. The color shades show the temperature field, black and white lines show ω -isolines ($\omega = 0.5, 1, 5, 20$ and 50) and ψ -isolines (values are shown on the line), respectively. (For interpretation of the references to color in this figure legend, the reader is referred to the web version of this article.)

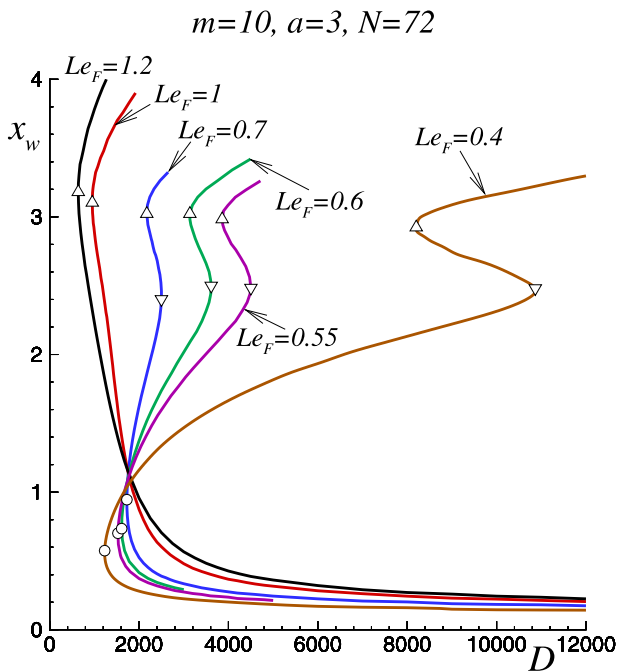


Fig. 5. Dependence of the edge flame position on the Damköhler number calculated for various decreasing Lewis numbers, for $m = 10$, $a = 3$ and $N = 72$ ($\beta = 10$). Turning points are marked with open symbols.

however, that the qualitative behavior of the response curves remains similar.

It can be seen in Fig. 9 that the branches corresponding to flame positions closer to the porous plug almost overlap for different values of a , while for branches with large x_w this does not happen. This behavior can be explained as follows. For the first solutions, the edge flame is located in the zone where the mixing of the reactants is just beginning. The mixture between the edge flame and porous plug is thus stoichiometric and complete combustion of both fuel and oxidizer occurs just behind the edge flame. For solutions with larger x_w , the

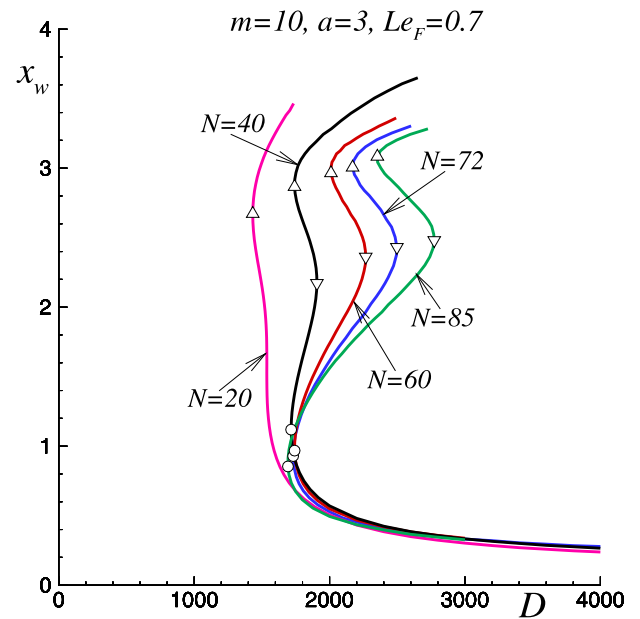


Fig. 6. Dependence of the edge flame position on the Damköhler number calculated for various values of the dimensionless activation energy N , for $m = 10$, $a = 3$ and $Le_F = 0.7$.

fuel and oxidizer are already partially premixed ahead the edge flame location. Then the mixture just upstream the edge flame is no longer stoichiometric and the scaling using β^3 becomes less adequate. Finally, Fig. 10 shows a map of the number of solutions in the $D - a$ plan. The digit inside each zone indicates the number of steady-state solutions.

It is interesting to note the following fact: if we gradually increase the value of the Damköhler number, we can see in Fig. 9 that for small values of a (e.g. the curve plotted for $a = 2$), solutions first arise with x_w located close to the porous plug. However, for large values of a (e.g. the curve plotted with $a = 7$) the first solutions that appear at small D are far from the porous plug. This is illustrated by the vertical dotted lines shown in Fig. 9 for the bifurcation points corresponding to the

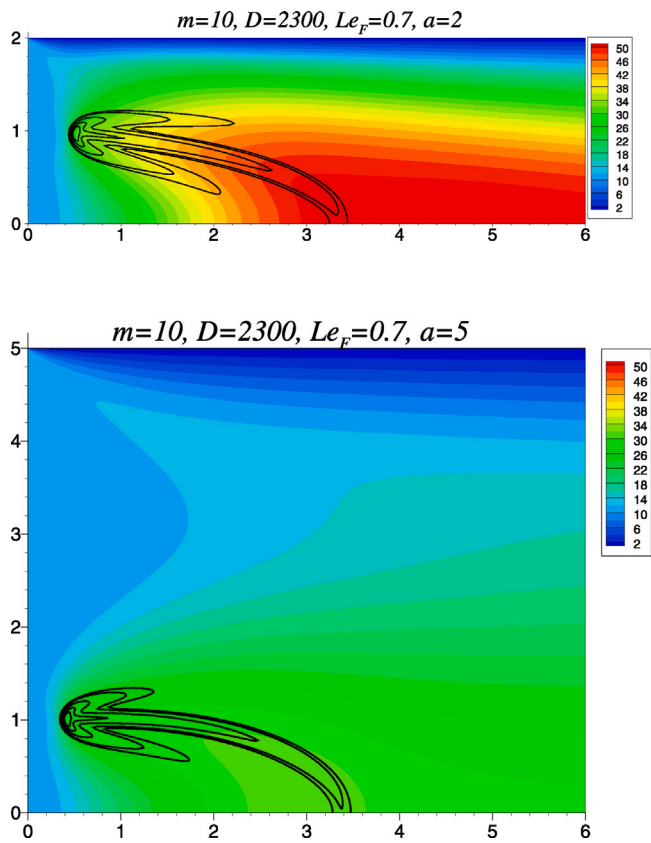


Fig. 7. Distributions of longitudinal velocity u for $D = 2300$, $m = 10$, $Le_F = 0.7$ in two cases with $a = 2$ and $a = 5$ (color shades), together with isolines of the omega reaction rate ($\omega = 0.5, 1, 5, 20, 50$). (For interpretation of the references to color in this figure legend, the reader is referred to the web version of this article.)

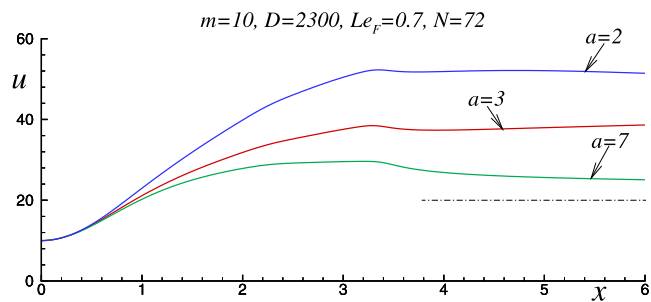


Fig. 8. Velocity profiles along the channel axis for $m = 10$, $D = 2300$, $Le_F = 0.7$ and three values of a . The dashed line marks the limit value of the velocity at the channel axis $u = 2m$.

remote solutions. In Fig. 10 this leads to the intersection of the curve with circles and the curve with triangles at $a \approx 5$.

5. Conclusions and discussions

The study of the phenomenon of multiplicity of operation modes of a device, when different regimes may simultaneously exist for a single set of parameters, is an important part of the design and feasibility studies of the system. Indeed, transition from one mode to another with a slight change in the control parameters may be undesirable when operating the device. It is important to note that careful numerical determination of the boundaries of the regions of multiplicity, or bifurcation points, requires the calculation of both stable and unstable steady states. For this reason, the direct application of a time-marching procedure perhaps is not effective, and special calculation methods must be used.

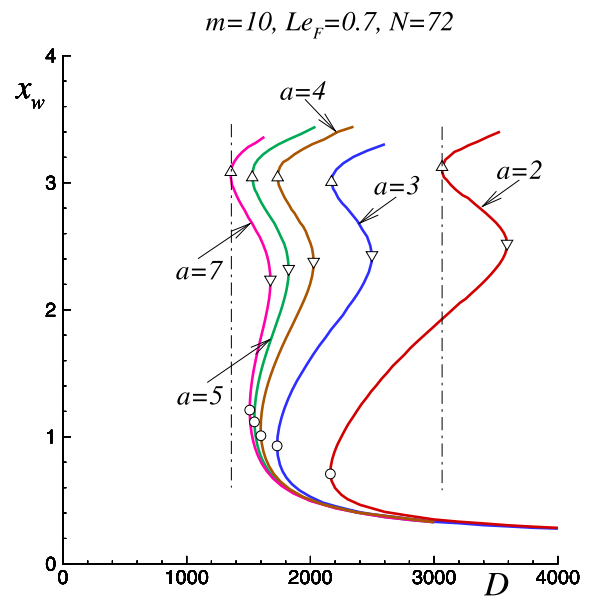


Fig. 9. Dependence of the edge flame position on the Damköhler number calculated for various dimensionless channel radius a , for $m = 10$, $Le_F = 0.7$ and $N = 72$ ($\beta = 10$). Open symbols indicate bifurcation points.

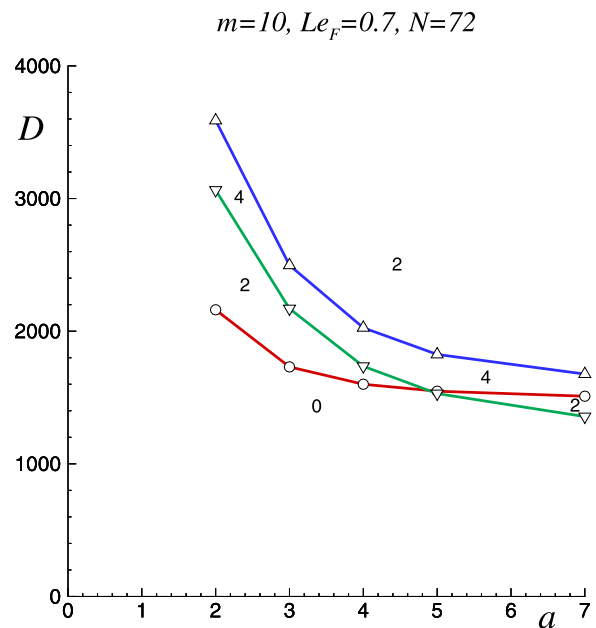


Fig. 10. Map of the multiplicity of steady-state modes in the $D - a$ parameters plane, calculated for $m = 10$, $Le_F = 0.7$ and $N = 72$. The numbers indicate the number of non-trivial solutions in each area (excluding the trivial cold solution $\theta \equiv 0$).

An obvious example of transition from one regime to another with only a small change in the parameter values is the flame extinction, since the trivial cold state is also one of the possible modes. A less obvious example is the transition from one combustion mode to another, different in the flame structure, combustion characteristics and interaction with the environment. This case is investigated in the present study for a combustion device with separate injection of fuel and oxidizer into the combustion chamber.

The present numerical study reveals the possibility of multiple edge flame solutions as a circular fuel jet is injected in the middle of a circular channel separately from a surrounding oxidizer stream. The study focuses in a simplified case of injection through a highly

conducting porous plug, ensuring uniform flux of reactants at a uniform temperature, and considers only axisymmetric solutions.

Results show that two different axisymmetric solutions may exist for unity fuel Lewis number flames. As the fuel Lewis number decreases, up to four different axisymmetric flames solutions are found, with two of them being in all probability simultaneously stable. These investigations could be important in light of the current increasing interest in the study of designs for burning hydrogen, including that obtained from renewable sources, for domestic and industrial purposes.

Perhaps these results may open the way to an explanation for experimental observations reporting an alternance of anchored and lifted flames in axial non-premixed burners [25], particularly when burning fuels with $Le_F < 1$. One has to bear in mind that, in addition to multiple axisymmetric flames, non-axisymmetric solutions, both stable and unstable, must certainly also exist for the same parameters, as was the case in the planar jet studies reported in [23,24]. This shall be investigated in future work.

CRediT authorship contribution statement

Vadim N. Kurdyumov: Investigation. **Carmen Jiménez:** Investigation.

Declaration of competing interest

The authors declare that they have no known competing financial interests or personal relationships that could have appeared to influence the work reported in this paper.

Acknowledgments

The authors would like to express their gratitude to Thierry Schuller from IMFT (France) for his participation in the problem formulation. This study was supported by MCIN with funding from European Union NextGenerationEU (PRTR-C17.I1) as well by grants #TED2021-129446-C42/MCIN/AEI/10.13039/501100011033/NextGenerationEU/PRTR and #PID2022-139082NB-C52 MCIN/AEI/10.13039/501100011033/ and FEDER.

References

- [1] N. Peters, Local quenching due to flame stretch and non-premixed turbulent combustion, *Combust. Sci. Technol.* 30 (1983) 1–17.
- [2] J. Buckmaster, M. Matalon, Anomalous Lewis number effect in tribranchial flames, *Symp. (Int.) Combust.* 22 (1988) 1527–1535.

- [3] J. Buckmaster, Edge-flames and their stability, *Combust. Sci. Technol.* 115 (1996) 41–68.
- [4] J. Buckmaster, Edge-flames, *Prog. Eng. Combust.* 28 (2002) 435–475.
- [5] V.N. Kurdyumov, M. Matalon, Radiation losses as a driving mechanism for flame oscillations, *Proc. Combust. Inst.* 29 (2002) 45–52.
- [6] V.N. Kurdyumov, M. Matalon, Dynamics of an edge flame in a mixing layer, *Combust. Flame* 139 (2004) 329–339.
- [7] V.N. Kurdyumov, M. Matalon, Stabilization and onset of oscillation of an edge-flame in the near-wake of a fuel injector, *Proc. Combust. Inst.* 31 (2007) 909–917.
- [8] V. Kurdyumov, M. Matalon, Effects of thermal expansion on the stabilization of an edge-flame in a mixing-layer model, *Proc. Combust. Inst.* 32 (2009) 1107–1115.
- [9] J.A. Bieri, M. Matalon, Edge flames stabilized in a non-premixed microcombustor, *Combust. Theor. Model.* 15 (2011) 911–932.
- [10] J.A. Bieri, V.N. Kurdyumov, M. Matalon, The effect of gas expansion on edge flames stabilized in narrow channels, *Proc. Combust. Int.* 33 (2011) 1227–1234.
- [11] K.-P. Liao, M. Matalon, C. Pantano, A flow pattern that sustains an edge flame in a straining mixing layer with finite thermal expansion, *Proc. Combust. Inst.* 35 (2015) 1015–1021.
- [12] B. Shields, J.B. Freund, C. Pantano, Stationary edge flames in a wedge with hydrodynamic variable-density interaction, *Combust. Flame* 211 (2020) 347–361.
- [13] E. Fernandez-Tarrazo, M. Vera, A. Liñán, Liftoff and blowoff of a diffusion flame between parallel streams of fuel and air, *Combust. Flame* 144 (2006) 261–276.
- [14] V.N. Kurdyumov, M. Matalon, Dynamics of an edge-flame in the corner region of two mutually perpendicular streams, *Proc. Combust. Inst.* 31 (2007) 929–938.
- [15] G.R. Ruetsch, L. Vervisch, A. Liñán, Effects of heat release on triple flames, *Phys. Fluids A* 7 (1995) 1447–1454.
- [16] J. Daou, A. Liñán, The role of unequal diffusivities in ignition and extinction fronts in strained mixing layers, *Combust. Theor. Model.* 2 (1998) 449–477.
- [17] S. Ghosal, L. Vervisch, Theoretical and numerical study of a symmetrical triple flame using the parabolic flame path approximation, *J. Fluid Mech.* 415 (2000) 227–260.
- [18] V. Nayagam, F. Willams, Lewis-number effects in edge-flame propagation, *J. Fluid Mech.* 458 (2002) 219–228.
- [19] R.W. Thatcher, A.A. Omon-Arancibia, Multiple speeds of flame edge propagation for Lewis numbers above one, *Combust. Theor. Model.* 9 (2005) 647–658.
- [20] M.S. Cha, P.D. Ronney, Propagation rates of nonpremixed edge flames, *Combust. Flame* 146 (2006) 312–328.
- [21] J. Daou, F. Al-Malki, Triple-flame propagation in a parallel flow: an analytical study, *Combust. Theor. Model.* 14 (2010) 177–202.
- [22] P. Pearce, J. Daou, The effect of gravity and thermal expansion on the propagation of a triple flame in a horizontal channel, *Combust. Flame* 160 (2013) 2800–2809.
- [23] V.N. Kurdyumov, C. Jiménez, Lifted jet edge flames: symmetric and non-symmetric configurations, *Combust. Theor. Model.* 26 (2022) 1114–1129.
- [24] C. Jiménez, V.N. Kurdyumov, Multiplicity of solutions of lifted jet edge flames: Symmetrical and non-symmetrical configurations, *Combust. Flame* 256 (2023) 112988.
- [25] S. Marragou, H. Magnes, A. Aniello, L. Selle, T. Poinso, T. Schuller, Experimental analysis and theoretical lift-off criterion for H₂/air flames stabilized on a dual swirl injector, *Proc. Combust. Inst.* 39 (2023) 4345–4354.